

A FRF-based algorithm for damage detection using experimentally collected data

Antonio Garcia-Palencia¹, Erin Santini-Bell^{*2}, Mustafa Gul³ and Necati Catbas⁴

¹HNTB Corporation, Boston, MA 02116, USA

²Department of Civil Engineering, University of New Hampshire, Durham, NH 03824, USA

³Department of Civil and Environmental Engineering, University of Alberta, Edmonton, AB T6G 2W2, Canada

⁴Department of Civil and Environmental and Construction Engineering, University of Central Florida, Orlando, FL 32816, USA

(Received July 29, 2015, Revised November 20, 2015, Accepted November 27, 2015)

Abstract. Automated damage detection through Structural Health Monitoring (SHM) techniques has become an active area of research in the bridge engineering community but widespread implementation on in-service infrastructure still presents some challenges. In the meantime, visual inspection remains as the most common method for condition assessment even though collected information is highly subjective and certain types of damage can be overlooked by the inspector. In this article, a Frequency Response Functions-based model updating algorithm is evaluated using experimentally collected data from the University of Central Florida (UCF)-Benchmark Structure. A protocol for measurement selection and a regularization technique are presented in this work in order to provide the most well-conditioned model updating scenario for the target structure. The proposed technique is composed of two main stages. First, the initial finite element model (FEM) is calibrated through model updating so that it captures the dynamic signature of the UCF Benchmark Structure in its healthy condition. Second, based upon collected data from the damaged condition, the updating process is repeated on the baseline (healthy) FEM. The difference between the updated parameters from subsequent stages revealed both location and extent of damage in a “blind” scenario, without any previous information about type and location of damage.

Keywords: damage detection; dynamic nondestructive testing; bridges; frequency response functions; finite element models; model updating

1. Introduction

Currently, condition assessment of in-service bridges is primarily based on visual inspection to evaluate their structural integrity; this basically means that “what you see is what you get”. However, visual inspection has two major disadvantages. First, certain types of damage can be hidden from view, for example internal cracking in beams or under asphalt membranes. Second, visual inspection can be extremely difficult to perform in some instances, for example, in long bridges spanning waterways. A hands-on detailed visual inspection for a typical overpass bridge can take about 3 hours whereas the vibration signature of a properly instrumented bridge can be

*Corresponding author, Professor, E-mail: erin.bell@unh.edu

collected in the same time frame.

Although, additional time for data post-processing is required, the vibration signature provides more objective information about the structural condition and can be tracked over time to detect changes that may not be visible to the human eye. Also, it should be noted that the vibration based monitoring can be conducted much more frequently than the visual inspection once the bridge is instrumented.

In response to the current infrastructure concerns (American Society of Civil Engineers, 2013), more attention has been drawn to the application of SHM methods as a tool for condition assessment in the context of civil engineering infrastructure. SHM is composed of four damage identification levels (Rytter 1993): 1) Detection, 2) localization, 3) quantification and 4) prediction of remaining life. Most of the methods developed to date for large scale systems can only attain levels 1 and 2 given the many challenges on modelling, data collection and especially post processing as measurements are highly dependent on environmental conditions (Chesné and Deraemaeker 2013). By integrating SHM systems to the current visual inspection protocols, a better damage diagnosis in properly instrumented bridges can be attained.

Vibration-based methods for SHM have received considerable attention during the last two decades, since dynamic data is global in nature and easier to collect in the field. A detailed review on this subject is presented in (Hsieh *et al.* 2006, Cruz and Salgado 2008, Fan and Qiao 2011, Talebinejad *et al.* 2011, Chesné and Deraemaeker 2013). This research focuses on Model Based (MB) methods, which rely on a Finite element Model (FEM) to evaluate the condition of in-service structures.

Essentially, MB methods require an error function that expresses the difference between analytically predicted and experimentally measured response (Mottershead and Friswell 1993). Then, that error function is minimized based on selected unknown structural parameters based on field observations and engineering judgment. This process is widely known as model updating. As a result, a multi-stage approach is implemented in order to assess structural health. First, the initial FEM is updated via changes in stiffness, mass and damping parameters, in order to capture the dynamic signature of the structure in its undamaged state (i.e., baseline model). Then the updating process is repeated for each set of vibration measurements from different damage states as required by the SHM system, with damage defined as meaningful changes to the stiffness, mass and damping matrices of the structure. The difference between updated parameters from the baseline and subsequent damage states can be used to locate and quantify damage.

Recently, researchers have developed methods based on modal information (Mendrok and Uhl 2010, Jafarkhani and Masri 2011, Panigrahi *et al.* 2013, Modak 2014, Wang *et al.* 2014) and Frequency Response Functions (Esfandiari *et al.* 2009, Maia *et al.* 2011, Rahmatalla *et al.* 2012, Chesné and Deraemaeker 2013, Gang *et al.* 2014). While using modal data has been the most commonly employed approach for model updating given its many advantages (Ewins 2000), information is limited to that at resonance and could be prone to extraction errors. On the other hand, FRF-based techniques bypass such extraction errors while providing information in a frequency-by-frequency basis. However, dealing with FRFs has some disadvantages because they are more complex mathematically and such methods could be computationally very expensive for large-scale structures. Additionally, (Catbas *et al.* 2012) showed that practical technologies (e.g., Falling Weight Deflectometer) can be utilized to generate input-output data

The previous publications on this FRF-based two-step model updating algorithm presented the mathematical formulation and calibration of a FEM of the UCF Benchmark (Garcia-Palencia and Santini-Bell 2013), and the Powder Mill Bridge (Garcia-Palencia *et al.* 2014). In both cases,

parameter identification was performed on the baseline (undamaged) model only. In this article, the model updating algorithm is extended to include damage detection, localization and quantification using experimentally obtained FRF data. In addition, a regularization technique and a protocol for selection of frequency points for updating is developed in this work in order to provide the most well-conditioned model updating scenario for the target structure.

The target structure is the University of Central Florida (UCF) Benchmark (Gul 2009) and is intended to capture the dynamic behavior of short to medium span bridges. Several boundary conditions (e.g., rollers, fixed support and semi fixed support with neoprene pads) can be set in order to simulate different damage cases. This is a collaborative effort between several academic institutions and first started under the auspices of the International Association for Bridge Maintenance and Safety (IABMAS) (Caicedo *et al.* 2006, Catbas *et al.* 2006, Cruz and Salgado 2008).

2. Frequency response functions-based model updating for damage detection

In this study, model updating is performed using a FRF-based error function proposed originally by Thyagarajan *et al.* (1998). This formulation was further modified by Garcia-Palencia and Santini-Bell (2013) to account for multiple excitation points and with a damping matrix that captures the variation of modal damping ratios with natural frequencies. A summary of the formulation for model updating is presented here for completeness and clarity.

The equation of motion of a viscously damped system subjected to a harmonic force can be expressed as shown in Eq. (1) (Thyagarajan *et al.* 1998).

$$[M]\{\ddot{u}\} + [C]\{\dot{u}\} + [K]\{u\} = \text{Re}(\{F\}e^{j\Omega t}) \quad (1)$$

where $[K]$, $[M]$ and $[C]$ are the stiffness, mass and damping matrices respectively, $\{u\}$ is the displacement vector, Ω is the frequency of the excitation load, $\{F\}$ is a vector that contains the amplitude of the applied forces, $j = \sqrt{-1}$, and t is the time. A solution of Eq. (1) is given by

$$\{u(t)\} = \text{Re}(\{q\}e^{j\Omega t}) \quad (2)$$

where $\{q\}$ is a complex frequency response vector. Substitution of Eq. (2) into Eq. (1) gives

$$\text{Re} \left[\left(([K] - \Omega^2[M] + j\Omega[C])\{q\} - \{F\} \right) e^{j\Omega t} \right] = 0 \quad (3)$$

A solution to Eq. (3) is given by

$$([K] - \Omega^2[M] + j\Omega[C])\{q\} - \{F\} = 0 \quad (4)$$

Assume that modal testing is performed on the structure and the FRF vector $\{q_e\}$ are the measured displacements. Let the dynamic stiffness matrix $[A] = [K] - \Omega^2[M] + j\Omega[C]$ and $\{q_e\} = \{q_a \ q_b\}^T$, where q_a and q_b represent degrees of freedom (dofs) on the real structure where the FRFs are measured and not measured respectively. The matrix $[A]$ can also be partitioned accordingly as shown in Eq. (5)

$$[A] = \begin{bmatrix} A_{aa} & A_{ab} \\ A_{ba} & A_{bb} \end{bmatrix} = \begin{bmatrix} K_{aa} - \Omega^2 M_{aa} + j\Omega C_{aa} & K_{ab} - \Omega^2 M_{ab} + j\Omega C_{ab} \\ K_{ba} - \Omega^2 M_{ba} + j\Omega C_{ba} & K_{bb} - \Omega^2 M_{bb} + j\Omega C_{bb} \end{bmatrix} \quad (5)$$

After some mathematical manipulations, the FRF-based two-step error function $\{e_{FRF}(p_1, p_2)\}$ for any frequency Ω_r is given by Eq. (6). For an interested reader, a detailed derivation is given in (Garcia-Palencia and Santini-Bell 2013)

$$\{e_{FRF}(p_1, p_2)\} = \left[([A_{aa}] - [A_{ab}][A_{bb}]^{-1}[A_{ba}])\{q_a\} - (\{F_a\} - [A_{ab}][A_{bb}]^{-1}\{F_b\}) \right]_{\Omega=\Omega_r} \quad (6)$$

where $\{p_1\}$ includes the unknown properties of the system such as modulus of elasticity and mass density, that are related to $[K]$ and $[M]$; $\{p_2\}$ includes the unknown damping parameters which are related to $[C]$ and $\{F_a\}$ and $\{F_b\}$ are the result of partitioning the vector of applied forces $\{F\}$.

As it can be observed in Eq. (6), multiple inverse calculations are required when computing the error vector for scenarios with sparse measurements. Solving a complex matrix inverse can be particularly computationally intensive. In this research, a single object oriented solver called *Factorize* (Davis 2013) is integrated into the model updating algorithm. *Factorize* improves how rank-deficient systems are handled by incorporating a complete orthogonal decomposition, and the singular value decomposition.

Model updating is performed in two steps: in Step 1, only the mass and stiffness matrices will be updated therefore $\{p_1\}$ is set as the vector of unknown parameters and $\{p_2\}$ is kept constant. In other words, the modal damping ratios remain unchanged from the initial numerical model. On the other hand, in Step 2 the damping matrix will be updated and $\{p_2\}$ is set as the new vector of unknown parameters, while keeping the updated parameters from Step 1 $\{p_1\}^{updated}$ as constants. Different segments of the frequency response function provide meaningful information about different parameter groups, specifically (1) stiffness and mass and (2) damping. By developing a two-step model updating protocol, frequency points can be selected to provide the most well-conditioned model updating scenario for each target structure. A frequency selection protocol is presented in Sections 4.1.1 and 4.1.2. Therefore, Eq. (6) can be rewritten as shown in Eq. (7); for the sake of consistency, $\{p_2\}^*$ denotes the initial damping parameter vector that is kept constant for Step 1

$$\{e_{FRF}(p_1, p_2^*)\} = \left[([A_{aa}] - [A_{ab}][A_{bb}]^{-1}[A_{ba}])\{q_a\} - (\{F_a\} - [A_{ab}][A_{bb}]^{-1}\{F_b\}) \right]_{\Omega=\Omega_r} \quad (7)$$

Likewise, Eq. (6) can be modified for Step 2 where the damping matrix will be updated and $\{p_2\}$ is set as the new vector of unknown parameters. Updated parameters from Step 1 $\{p_1^{updated}\}$ will be kept constant then

$$\{e_{FRF}(p_1^{updated}, p_2)\} = \left[([A_{aa}] - [A_{ab}][A_{bb}]^{-1}[A_{ba}])\{q_a\} - (\{F_a\} - [A_{ab}][A_{bb}]^{-1}\{F_b\}) \right]_{\Omega=\Omega_r} \quad (8)$$

The stacked residual error vector for the k th dynamic test $\{E_I(p)_k\}$ is calculated as shown in Eq. (9)

$$\{E_I(p)_k\} = \begin{Bmatrix} e_{FRF}(p)_{\Omega_1} \\ \vdots \\ e_{FRF}(p)_{\Omega_{r-1}} \\ e_{FRF}(p)_{\Omega_r} \end{Bmatrix} \quad (9)$$

where $\{e_{FRF}(p)_{\Omega_r}\}$ is the error vector for the r th updating frequency Ω_r , and is a function of the unknown parameters $\{p\}$. Depending on the step, $\{p\}$ can be either $\{p_1\}$ or $\{p_2\}$. In turn, the stacked error vector $\{E_{FRF}(p)\}$ that accounts for different load locations $\{E_I(p)_k\}$ is given by Eq. (10)

$$\{E_{FRF}(p)\} = \{E(p)\} = \begin{Bmatrix} E_I(p)_1 \\ \vdots \\ E_I(p)_{k-1} \\ E_I(p)_k \end{Bmatrix} \tag{10}$$

Essentially, parameter estimation through model updating is a constrained minimization problem. Then, the error function $\{E(p)\}$ has to be expressed as a scalar objective function $J(p)$

$$J(p) = \{E(p)\}^{*T} \{E(p)\} \tag{11}$$

where the superscript $*T$ is the conjugate transpose of the error the vector. The associated minimization problem from Eq. (11) can be expressed as Eq. (12)

$$\min J(p) \text{ subject to } \{p_{min}\} < \{p\} \leq \{p_{max}\} \tag{12}$$

where $\{p_{min}\}$ and $\{p_{max}\}$ are predefined constrains based on engineering judgment. Such constrains prevents the search algorithm from generating physically meaningless solutions.

In some cases, optimization can be particularly challenging due to measurement errors and ill-conditioning. Regularization techniques (Tikhonov and Arsenin 1977, Weber *et al.* 2009, Fu *et al.* 20113) partially address these issues by adding new information in the form of a side constraint (Mottershead *et al.* 2011)

$$J(\{p\}) = \{E(\{p\})\}^T [W_E] \{E(\{p\})\} + \gamma^2 \{\Delta p_i\}^T [W_\theta] \{\Delta p_i\} \tag{13}$$

where the regularization parameter γ provides a balance between the objective error function $J(\{p\}) = \{E(\{p\})\}^T [W_E] \{E(\{p\})\}$ and the side constraint $\{\Delta p_i\}^T [W_\theta] \{\Delta p_i\}$. Link (1993), suggests that γ^2 should lie in the range from 0 (no regularization) and 0.3, for strong ill-conditioning. In this article, $\gamma^2 = 0.05$ is used as suggested by Mottershead *et al.* (2011). The matrix $[W_\theta]$ can be expressed as (Link 1993)

$$[W_\theta] = \frac{\text{mean}(\text{diag}([\Gamma]))}{\text{mean}(\text{diag}([\Gamma]^{-1}))} [\Gamma]^{-1} \quad ; \quad [\Gamma] = \text{diag}[S(\{p\})^T [W_E] [S(\{p\})]] \tag{14}$$

where $[S(\{p\})]$ is a sensitivity matrix where each column represents the partial derivative of $\{E(\{p\})\}$ with respect to each unknown parameter from $\{p\}$. Eq. (14) constrains $\{\Delta p_i\}^T$ according to their sensitivities so that parameters remain unchanged if the sensitivity approaches zero. For a least-squares solution, the change in parameter $\{\Delta p_i\}$ for the FRF error function is calculated based on Mottershead *et al.* (2011) as

$$\{\Delta p_i\} = \text{Re} \left(- \left[[S(\{p\})]^{*T} [W_E] [S(\{p\})]^T + \lambda^2 [W_\theta] \right]^{-1} [S(\{p\})]^{*T} [W_E] \{E(\{p\})\} \right) \tag{15}$$

In this research, MUSTANG, (Model Updating STRUCTURAL ANALYSIS proGram) a MATLAB-based (MathWorks Inc., 2011) iterative algorithm developed at the University of New Hampshire, is used to minimize $J(\{p\})$. MUSTANG is linked to SAP2000 (Computers and Structures, Inc., 2011) through its Application Programming Interface (API) and allows the user to perform model updating at predefined groups of elements.

3. Description of the target structure: The UCF-Benchmark

The University of Central Florida (UCF) Benchmark Structure (Fig. 1) was used to validate the model updating methodologies presented in this article. The structure was intended to capture the dynamic behavior of short to medium span bridges. A detailed description of the physical model is given in Burkett (2005) and Gul (2009).

The structure was constructed with steel sections and can be easily modified for different test setups. The dimensions are 5.49 m by 1.83 m with transverse bracing at 0.91 m intervals as shown in Fig. 2. Beams have S76x8.4 (S3x5.7) sections whereas the columns are W310x38.7 (W12x26). Also, several boundary conditions (e.g., pin support, rollers, fixed support and semi fixed support with neoprene pads) can be set in order to simulate different damage cases (Gul and Catbas 2008).



Fig. 1 Experimental setup of the UCF Benchmark Structure (adopted from Gul and Catbas 2008)

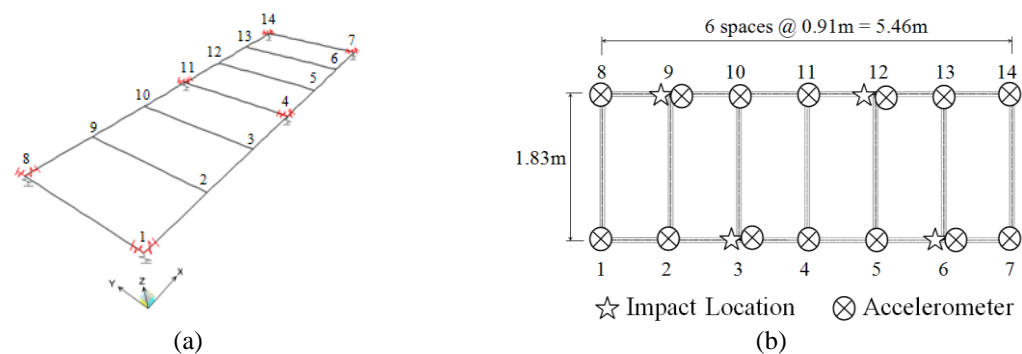


Fig. 2 (a) Finite Element Model using SAP2000[®] and (b) Plan view of the structure and instrumentation layout

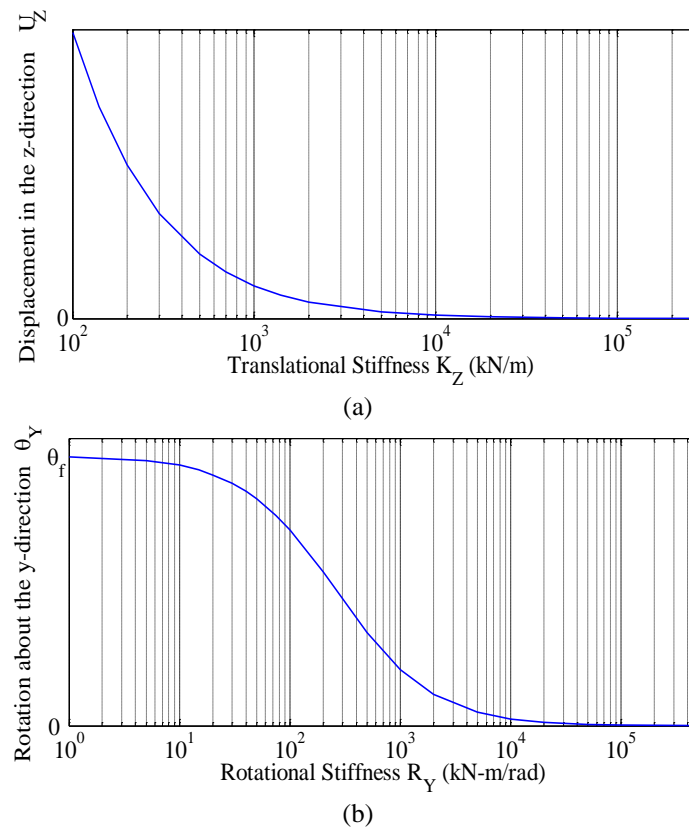


Fig. 3 Variation of boundary conditions with respect to displacements/rotations: (a) U_z vs. K_z and (b) θ_y vs. R_y

The initial FEM of the UCF Benchmark structure (Fig. 2(a)) was created in SAP2000® (Computers and Structures, Inc., 2011) and has 196 nodes and 201 frame elements with modulus of elasticity $E_{\text{STEEL}} = 200 \text{ GPa}$ and mass density $\rho_{\text{STEEL}} = 7850 \text{ kg/m}^3$. Additional translational and rotational springs at the corner joints 1, 4, 7, 8, 11 and 14 were added so that changes in the boundary conditions can be captured by the FEM during the model updating process. Initial values for the boundary conditions are based upon the plots shown in Fig. 3, and express the variation of the springs' stiffness with respect to the rotation/displacements at the node of interest.

They were obtained by applying an arbitrary static point load at node 3 on the FEM and then calculating the displacements U_z and the rotations θ_y at each support. As it can be observed in Fig. 3, the plots are generic as the values of displacements/rotations change depending on the support, but the values of the stiffness for free condition/full fixity are consistent for each support. Translational springs in the vertical direction were assumed as $K_z = 2 \times 10^5 \text{ kN/m}$ which represents fixity in the z -direction whereas rotational spring R_z and R_y are assumed as $1 \text{ kN}\cdot\text{m/rad}$. Those initial values are the “best guess” based upon as-built drawings and reflect the physical boundary conditions in the healthy structure (approximately pinned/roller connections). On the other hand, damping in the FEM was calculated by superposing modal damping matrices as shown in Eq. (16)

$$[C] = [M] \left(\sum_{n=1}^N \frac{2\zeta_n \omega_n}{M_n} \phi_n \phi_n^T \right) [M] \quad (16)$$

where ζ_n is the modal damping ratio of the n th mode shape ϕ_n , $M_n = \phi_n^T [M] \phi_n = 1$, ω_n is the n th natural circular frequency of vibration and N is the number of modes considered in the analysis. This damping formulation makes it possible to specify the modal damping ratios in any number of modes as opposed to Rayleigh damping or mass-proportional damping. Modal damping ratios of 0.15% are assumed for all the modes as a starting point for Step 1.

3.1 Dynamic testing on the UCF-Benchmark

Four separate impact tests were performed on the structure at selected locations and acceleration data were collected at 14 locations as shown in Fig. 2(b). However, accelerometers on the support nodes were not used in the calculations due to negligible vibration, which introduced excessive noise on the data. This reduces the number of measured nodes from 14 to eight. Based on the number of input and output location, the number of available FRFs for model updating is 32. These FRFs were obtained by using five averages. For the impact tests, an exponential window was applied to both input and output signals whereas a force window was applied only to the input signal. The sampling frequency was 320 Hz but the FRF analysis was carried out until 150 Hz because, according to the preliminary FE analysis, there were a sufficient number of modes in the range 0–150 Hz (Gul and Catbas 2008). Based upon experimental results evaluation data in the frequency range 5–110 Hz was selected for model updating, which corresponds to the first 12 modes of vibration as shown in Table 1.

4. Damage detection using experimentally obtained FRFs

In this study, damage detection through model updating is composed of two basic stages. First, the initial FEM of the UCF-Benchmark is updated via changes in stiffness, mass and damping parameters, in order to capture the dynamic signature of the system in its undamaged state (i.e. baseline model). Then, the updating process is repeated employing a new set of vibration measurements from the damaged configuration. In this research, damage was physically induced by fixing the support at nodes 7 and 14 with oversized through-bolts as observed in Fig. 4. The difference between updated parameters from the baseline and the subsequent damage state are used for damage detection. Results from the grouping strategies evaluated in this article clearly identified both the location and extent of the induced damage.

Table 1 Comparison of natural Frequencies from the initial FEM and Impact Data from experiments

	Natural Frequencies f_n (Hz)											
	f_1	f_2	f_3	f_4	f_5	f_6	f_7	f_8	f_9	f_{10}	f_{11}	f_{12}
FE	20.99	25.19	31.68	38.75	61.6	64.85	73.64	73.64	73.77	91.65	93.75	97.1
Impact	22.75	27.76	34.28	42.3	65.32	68.4	–	–	–	95.58	98.11	105.3



Fig. 4 Damaged support at nodes 7 and 14

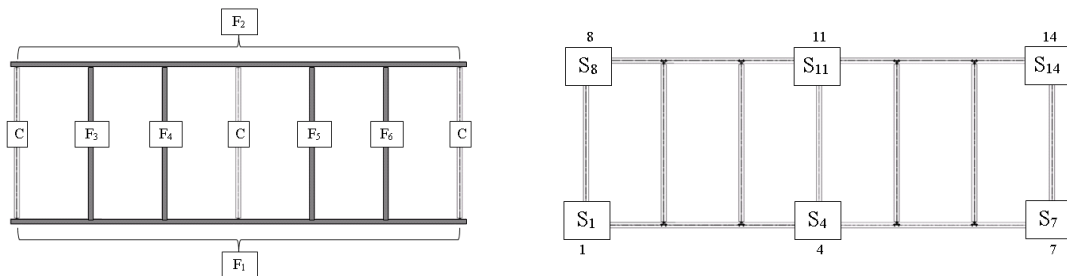


Fig. 5 Grouping strategies in the experimental study

The robustness of the algorithm to measurement errors was evaluated in a previous article (Garcia-Palencia *et al.* 2014), where the authors assumed 5% simulated random noise. In such study, the algorithm was able to detect, locate and quantify damage in boundary conditions with a 12.9% maximum error.

4.1 Baseline model

The initial FEM of the UCF-Benchmark will be updated using the proposed two-step approach introduced in Section 2. In Step one, $[K]$ and $[M]$ are updated by grouping unknown parameters that are expected to have similar properties so that the number of unknowns in the optimization problem can be reduced. The frame elements were subdivided into six groups (F_1 through F_6) for baseline generation purposes as shown in Fig. 5.

Such grouping strategy accounts for the inherent variability in the physical properties of the frames that occur from element to element. In addition, the measured FRFs must be sensitive to changes in the selected groups of unknown parameters in order to ensure successful model updating. For illustration purposes, the variation in FRF with respect to changes in E_{STEEL} , for group F_1 is presented in Fig. 6.

In this article, non-dimensional scalar multipliers applied at the element level (Mottershead *et al.* 2011) were used for model updating of the stiffness and mass parameters (α_K and β_M respectively). In other words, if for a given frame element $\alpha_K = 1.20$, this indicates a 20% increase

in frame’s stiffness. Frame elements labeled as “C” in Fig. 5 were kept constant during the optimization as well as the rotational stiffness R_Y , as they did not produce significant changes in the measured responses. As a result, the grouping strategy adopted in this article consists of six groups of frames and six groups of boundary conditions. The grouping strategy was illustrated in Fig. 5 and the number of unknowns is presented in Table 2.

Finally, appropriate selection of frequency points is another crucial aspect for successful updating of $[K]$ and $[M]$. Based upon results from Step 1, damping estimation is performed via changes in modal damping ratios using frequency points for updating located at resonance.

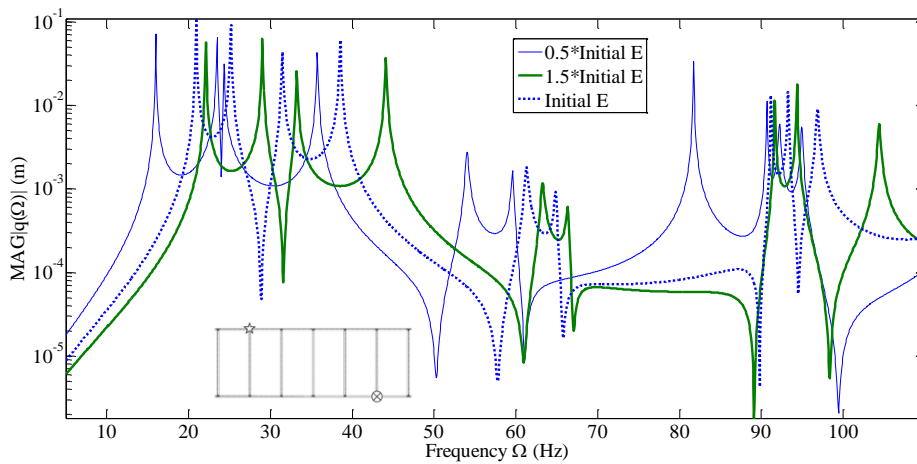


Fig. 6 FRF sensitivity to changes in E, frame group F_1

Table 2 Updated values of stiffness α_K , mass β_M and boundary conditions for the baseline (healthy) condition

Frame multipliers (unitless)					Boundary Conditions						
Group	α_K	Change (%)	β_M	Change (%)	Group	K_Z (kN/m)			R_Y (kN·m/rad)		
						Initial	Baseline	Change (%)	Initial	Baseline	Change (%)
F_1	1.21	21.0	1.03	3.0	S_1	200000	200000	0.00	1.00	1.00	0.0
F_2	1.22	22.0	1.02	2.0	S_4	200000	200000	0.00	1.00	23.69	2269
F_3	1.10	10.0	1.01	1.0	S_7	200000	200000	0.00	1.00	42.03	4103
F_4	1.11	11.0	1.00	0.0	S_8	200000	200000	0.00	1.00	1.00	0.0
F_5	1.15	15.0	1.06	6.0	S_{11}	200000	200000	0.00	1.00	18.70	1770
F_6	1.15	15.0	1.07	7.0	S_{14}	200000	200000	0.00	1.00	1.00	0.0

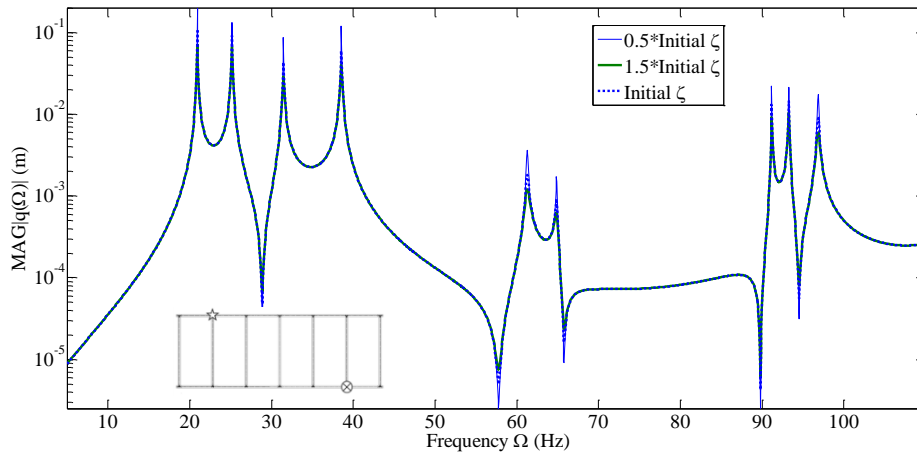


Fig. 7 FRF sensitivity to changes in damping

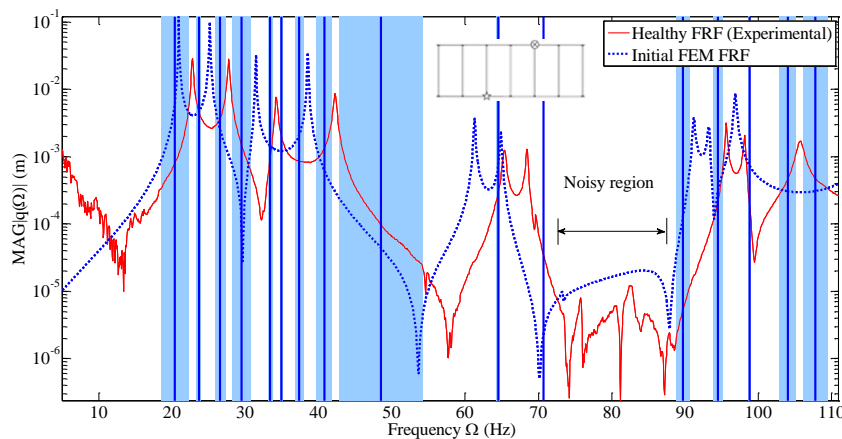


Fig. 8 Selection of frequency points for updating. The shaded regions are away from resonance, antiresonance and noisy areas while providing meaningful information for step 1

4.1.1 Updating $[K]$ and $[M]$ (Step 1)

In this step, updating is performed via changes in α_K , β_M and boundary conditions while keeping the initial modal damping ratios constant. Therefore, the presented methodology requires the selection of frequency points at locations that provide the most well-conditioned model updating scenario for each particular step. The goal of the two-step process is to “uncouple” the effects of Stiffness/Mass from damping parameters. For step 1, points should be located away from resonance and antiresonance areas, since damping parameters produce significant changes at such points (Kwon and Ling 2004, Esfandiari *et al.* 2009, Garcia-Palencia and Santini-Bell 2013) as illustrated in Fig. 7. In addition, noise-suspected regions on the measured FRFs should be avoided so that potential convergence issues can be reduced.

Once resonance, antiresonance and noise-suspected points were identified on each experimentally-measured FRF, frequency points located within ± 0.5 Hz were excluded from

updating. The remaining segments, depicted in Fig. 8 with shading, correspond to the potential set of frequency points for step 1 as shown with vertical lines in Fig. 8. The protocol is concluded by calculating the mid points on each identified segment, which provides sets of frequency points for updating promoting convergence to meaningful parameters.

Six groups of frames were considered in this model updating scenario. As a result, 12 frame parameters ($6\alpha_K + 6\beta_M$) and 12 unknown boundary conditions ($6K_Z + 6R_Y$) are set as unknown parameters, for a total of 24 unknowns in Step 1. Final parameter estimates are presented in Table 2; The updated stiffness parameters for element groups F_1 and F_2 showed the highest percent change during model updating. These element groups are similar in nature, being both external continuous members. Overall, maximum differences with respect to the initial values were 22% in α_K for group F_2 and 7% in β_M for group F_6 . As far as boundary conditions are concerned, the values of translational stiffness K_Z remain fixed with no change with respect to the initial values as observed in Fig. 9(a). The stiffness parameters for the boundary condition converged on values that reflected the pinned condition observed in the laboratory.

Finally, the maximum change in rotational stiffness R_Y occurred in joint 7, with an increase of 4103% with respect to the initial FEM resulting in a R_Y of 42.03 kN-m/rad, which is reflective of a pinned connection, as shown in Fig. 9(b). This is consistent with the construction observations. Fig. 10(a) shows the updated and experimental FRFs after Step 1 with predicted stiffness and mass parameters able to reproduce the experimental FRFs fairly well for frequencies up to 110Hz. The shift in the FRF amplitudes at resonance was corrected in Step 2 by adjusting modal damping ratios.

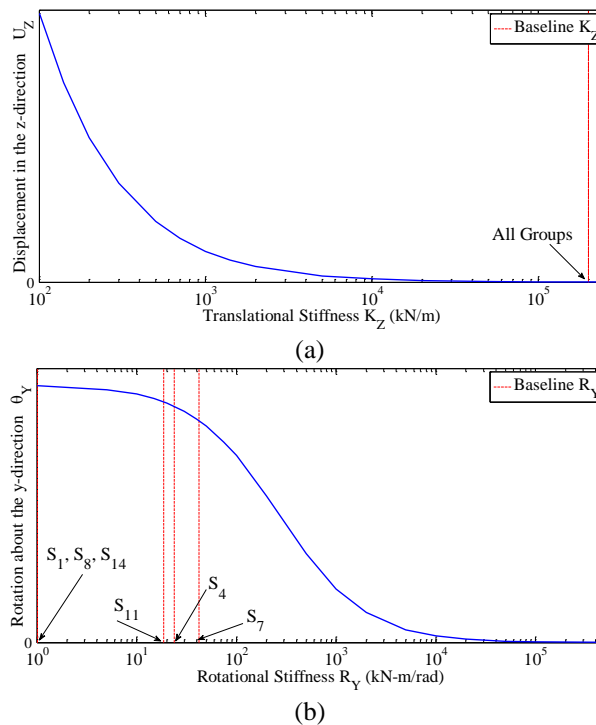


Fig. 9 Baseline boundary conditions (a) K_Z and (b) R_Y

4.1.2 Updating [C] (Step 2)

Identification of the damping matrix was performed via changes on the modal damping ratios while keeping [K] and [M] constant. In this step, minimization of the differences between the analytical and experimental FRFs was performed at selected resonant frequencies. As it was observed in Table 1, modes 7, 8 and 9 were not identified from the experimental FRFs due to the spatial resolution of the accelerometers and therefore the number of unknown modal damping ratios was set to 9.

Fig. 10(a) shows the updated and experimental FRFs that agree reasonably well in the frequency range [10–110] Hz. Initial and updated modal damping ratios are presented in Table 3, with initial values assumed as 0.15%. The maximum difference in modal damping ratios was 340.1% and corresponds to ζ_{12} .

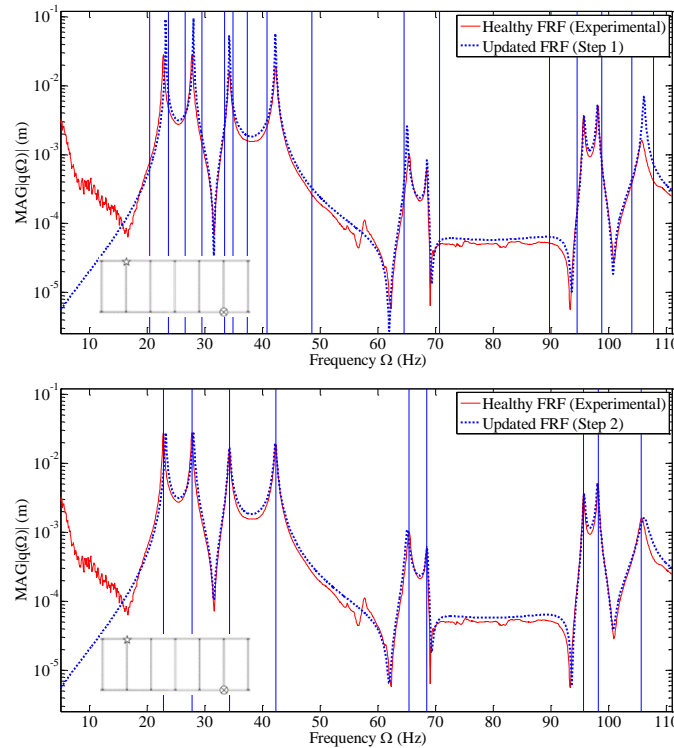


Fig. 10 Experimental and updated FRFs after Step 1 and 2

Table 3 Initial and Baseline (Healthy) modal damping ratios from Step 2

Damping ratio	ζ_1	ζ_2	ζ_3	ζ_4	ζ_5	ζ_6	ζ_7	ζ_8	ζ_9	ζ_{10}	ζ_{11}	ζ_{12}
Initial (%)	0.15	0.15	0.15	0.15	0.15	0.15	0.15	0.15	0.15	0.15	0.15	0.15
Baseline (%)	0.511	0.524	0.502	0.457	0.361	0.221	0.150	0.150	0.150	0.145	0.149	0.660
Change (%)	240.8	249.3	234.9	204.6	140.6	47.0	0.0	0.0	0.0	-3.2	-0.7	340.1

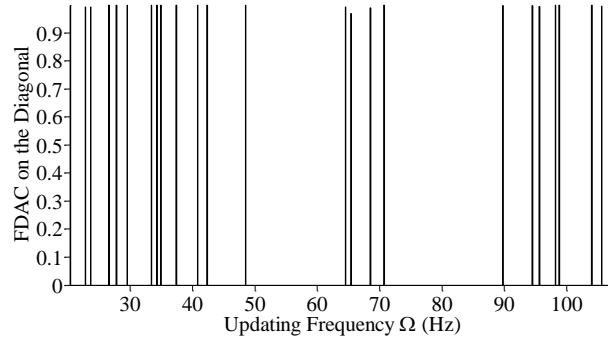


Fig. 11 Diagonal FDAC values for the baseline model and impact load at node 9

In this research, the quality of fit between experimental and predicted measurements was evaluated using the Frequency Domain Assurance Criterion (*FDAC*) (Pascual *et al.* 1996). For an impact location I the correlation between experimental FRFs $\{q_a\}$ and analytically predicted FRFs $\{q_p\}$ is calculated based upon Eq. (17)

$$FDAC(\Omega_p, \Omega_e)_I = \frac{\left| \{q_p(\Omega_p)\}^{*T} \{q_a(\Omega_e)\} \right|^2}{\left(\{q_p(\Omega_p)\}^{*T} \{q_p(\Omega_p)\} \right) \left(\{q_a(\Omega_e)\}^{*T} \{q_a(\Omega_e)\} \right)} \quad (17)$$

where Ω_e is the frequency at which $\{q_a\}$ was measured experimentally and Ω_p is the frequency at which $\{q_p\}$ was calculated from the FEM. Eq. (17) was evaluated for different frequency points, including those at resonance. *FDAC* values in the diagonal are presented in Fig. 11 where 1 indicates a perfect correlation. It is concluded that there exists a good agreement between both sets of FRFs, with *FDAC* values greater than 0.97. Similar plots were obtained for the other impact locations.

4.2 Damage detection

As mentioned before, extending this model updating method for damage detection is one of the unique contributions of this article. For validation purposes, structural damage was induced on the test structure by restraining two corner joints as indicated in Fig. 4. A new set of experimentally obtained FRFs (Fig. 12) was collected on the damaged configuration and the updating process will be repeated in order to achieve a Level 3 of damage identification (localization and quantification).

In order to be consistent with a real condition assessment scenario, the strategy for selecting the unknown parameters in the optimization should reflect the inability of a bridge inspector to identify damage location in advance. This “blind” strategy would suggest keeping the same unknown parameters used for baseline model generation. However, based on engineering judgment and previous research (Li *et al.* 2011) damage mostly affects the structure’s stiffness and the mass can be excluded from model updating. This reduces the unknown frame parameters to six groups of girders’ stiffness α_K .

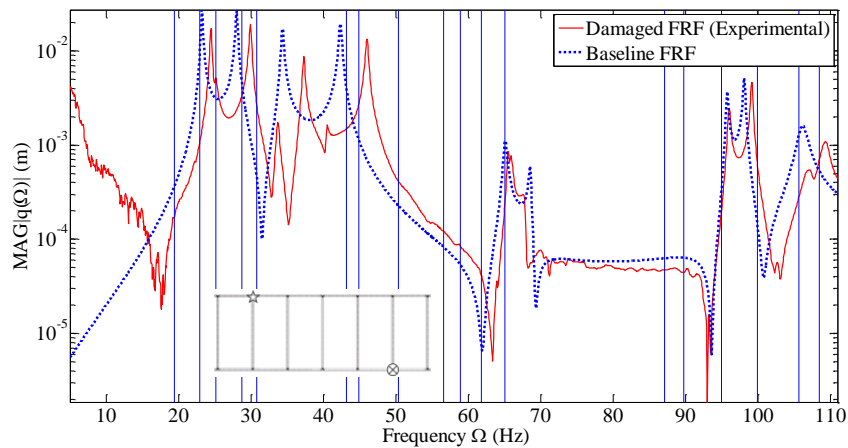


Fig. 12 Baseline and damaged FRFs

The difference between updated parameters from the baseline and the subsequent damage state revealed the location and extent of damage. Constraints on the optimization ensure that the frames' stiffness values α_K cannot increase from the undamaged model or decrease below zero. Finally, the upper bound for the translational stiffness K_Z is the initial value 2×10^5 kN/m as this represents fixity against vertical movement, as explained in explained in Section 3.

4.2.1 Updating $[K]$ (Step 1)

Selection of frequency points follows the same guidelines introduced in Section 4.1.1. Final parameter estimates are presented in Table 4 with predicted α_K values very similar to those from the baseline model with a maximum difference of -4.3% . This is consistent with the actual damage scenario as girders did not sustain any damage. As far as boundary conditions concerned, updated translational stiffness in all joints remained in their healthy condition (Fig. 13(a)) as well as the rotational stiffness in joints 1 and 4 (Fig. 13(b)).

However, even though joint 8 sought an increase of 482% in stiffness this is not indicative of damage as the value of R_Y for group S_8 remains very close to a pinned connection (Fig. 13(b)). Likewise, joint 11 sought an increase from 18.7 kN·m/rad to 42.51 kN·m/rad, which corresponds to a partially restrained joint but the value is still closer to pinned than it is to a fixed joint. Regardless of this “false positive”, the algorithm was able to clearly identify the actual location of damage in S_7 and S_{14} , as shown in Fig. 13(b). This plot revealed that the resulting R_Y values increased to reflect a fixed condition with a change of 697 % and 29393 % respectively. Such increase in stiffness is within the expected values for a fixed connection, therefore there is a high-confidence in the validity and uniqueness of the updated parameters. Finally, updated and damaged FRFs are shown in Fig. 14.

4.2.2 Updating $[C]$ (Step 2)

For the sake of completeness, model updating is concluded by calibrating the FRFs amplitudes at resonance, even though this step is not critical and do not provide any additional information that can be related to damage in the structure. Fig. 14 shows the updated and damaged FRFs for

Step 2. Again, the FRFs agree reasonably well in the frequency range [10–110] Hz whereas updated modal damping ratios are presented in Table 5. Finally, *FDAC* values are plotted in Fig. 15, which suggests a good agreement between both sets of FRFs with values in the diagonal greater than 0.90.

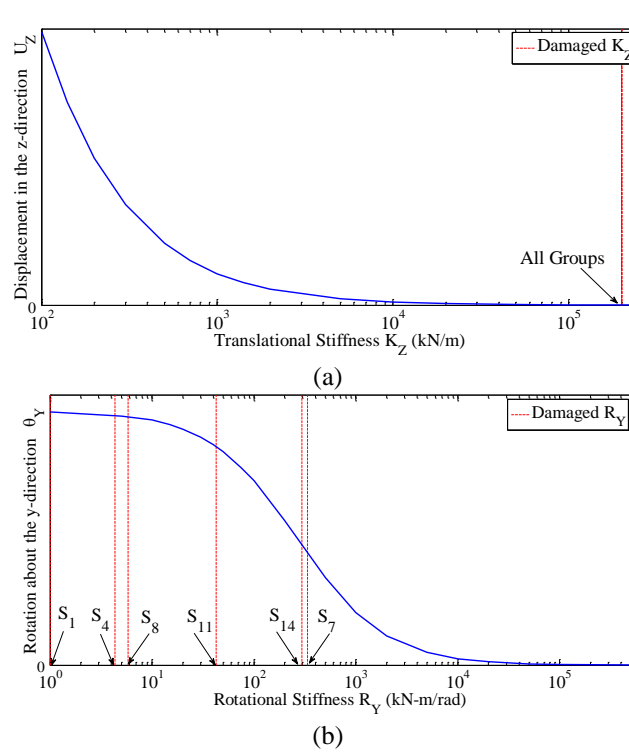


Fig. 9 Damaged boundary conditions (a) K_Z and (b) R_Y

Table 4 Updated values of stiffness and boundary conditions in the damaged conditions

Frame multipliers α_K (unitless)				Boundary Conditions						
Group	Healthy	Damaged	Change (%)	K_Z (kN/m)			R_Y (kN-m/rad)			
				Group	Healthy	Damaged	Change (%)	Healthy	Damaged	Change (%)
F ₁	1.21	1.25	3.2	S ₁	200000	200000	0.0	1.00	1.00	0.0
F ₂	1.22	1.17	-4.3	S ₄	200000	200000	0.0	23.69	4.31	-81.8
F ₃	1.10	1.10	0.0	S ₇	200000	200000	0.0	42.03	334.94	697
F ₄	1.11	1.10	-1.0	S ₈	200000	200000	0.0	1.00	5.82	482
F ₅	1.15	1.15	0.3	S ₁₁	200000	200000	0.0	18.70	42.51	127
F ₆	1.15	1.17	1.4	S ₁₄	200000	200000	0.0	1.00	294.93	29393

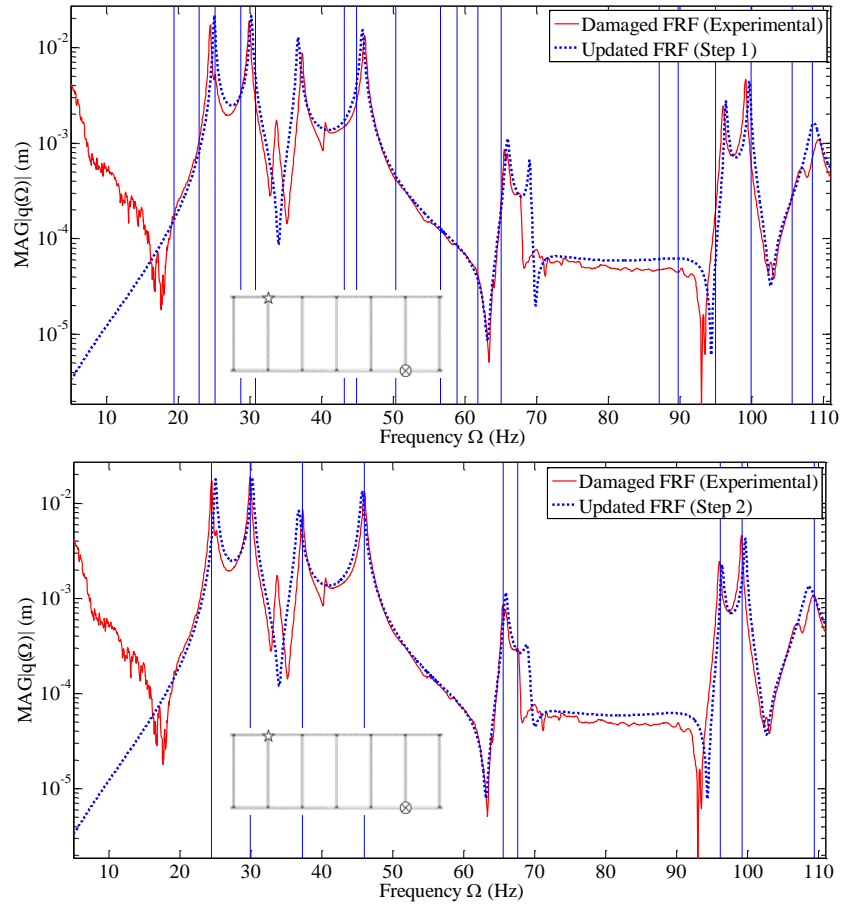


Fig. 14 Updated Baseline and damaged FRFs after Steps 1 and 2

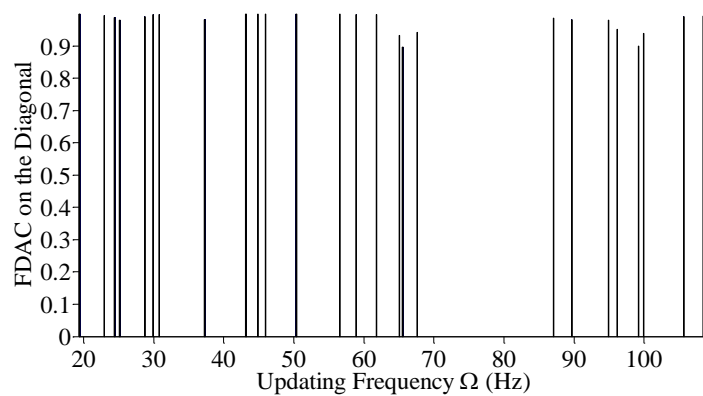


Fig. 15 Diagonal FDAC values for the damaged model for impact load at node 9

Table 5 Updated modal damping ratios from Step 2 from both GS-1 and GS-2

Damping ratio	ζ_1	ζ_2	ζ_3	ζ_4	ζ_5	ζ_6	ζ_7	ζ_8	ζ_9	ζ_{10}	ζ_{11}	ζ_{12}
Healthy	0.511	0.524	0.502	0.457	0.361	0.221	0.150	0.150	0.150	0.145	0.149	0.660
Updated	0.618	0.601	0.765	0.531	0.348	0.527	0.150	0.150	0.150	0.175	0.154	0.805
Change (%)	20.8	14.8	52.3	16.1	-3.5	138.9	0.0	0.0	0.0	20.6	3.2	21.9

5. Conclusions

This article presented a FRF-based algorithm for damage localization and quantification using experimentally collected data from the UCF-Benchmark Structure. The technique uses model updating to perform damage identification in two basic stages: First the initial FEM was updated via changes in stiffness, mass and damping parameters so that it captures the measured dynamic behavior in its undamaged state (i.e., baseline model).

Then the updating process was repeated using the data collected from the damaged structure with damage introduced by using oversized bolts at two corner joints. The difference between updated parameters from the baseline and the subsequent damage state was used to locate and quantify damage. This algorithm can be used as a complement to the current visual inspection protocols in order to improve the damage diagnosis in properly instrumented bridges. In addition, these updated models can be utilized for maintenance, retrofit as a result of the changed state of the bridge, which is objectively captured using measurements and also reflected in the updated models.

Baseline model updating is performed using a two-step procedure where stiffness and mass are calibrated in the first step and followed by damping identification. However, for damage detection purposes only stiffness and damping are updated as damage is not expected to affect $[M]$.

Selection of frequency points for updating is critical to ensure convergence and it is basically dependent on the updating step. For Step 1, frequency points should be located away from resonance, antiresonance and noisy areas on the experimentally measured FRFs whereas Step 2 requires points at resonance where modal damping parameters produce significant changes in the response. However, the frequency selection protocol is still dependent on the analyst's criterion which somehow makes the protocol subjective. For future research, a more automated protocol could be investigated in order to minimize the analyst's input.

The grouping strategy evaluated in this article consisted of six groups of frames and six groups of boundary conditions. The algorithm clearly identified the correct location of damage in a blind "scenario" by predicting an increase in rotational stiffness R_Y at the restrained joints with respect to the baseline or healthy values. Selection of parameters that produce significant changes in the measured FRFs is crucial for successful identification. Other important aspects include an appropriate grouping strategy of the unknown parameters and selection of constrains to ensure physically meaningful results.

Acknowledgements

The research presented here is based upon work supported by the National Science Foundation under Grant No. 0644683. Any opinions, findings, and conclusions or recommendations expressed in this material are those of the authors and do not necessarily represent the views of the National Science Foundation.

References

- American Society of Civil Engineers (2013), <http://www.infrastructurereportcard.org/bridges/>. [Online] [Accessed July 2014].
- Burkett, J.L. (2005), *Benchmark Studies for Structural Health Monitoring Using Analytical and Experimental Models*, M.S. Thesis University of Central Florida.
- Caicedo, J.M. et al. (2006), *Benchmark Problem for Bridge Health Monitoring: Definition Paper*, San Diego, California, USA, s.n.
- Catbas, F.N., Gokce, H.B. and Gul, M. (2012), "A practical methodology for load rating of existing highway bridges: demonstration on reinforced concrete T-beam bridges", *J. Bridge Eng.*, **17**(4), 652-661, ASCE do [http://dx.doi.org/10.1061/\(ASCE\)BE.1943-5592.0000284](http://dx.doi.org/10.1061/(ASCE)BE.1943-5592.0000284)
- Catbas, F.N., Caicedo, J.M. and Dyke, S.J. (2006), *Proceedings of the International Conference on Bridge Maintenance, Safety and Management, IABMS*, July 16-19, 2006. Porto, Portugal, s.n.
- Chesné, S. and Deraemaeker, A. (2013), "Damage localization using transmissibility functions: A critical review", *Mech. Syst. Signal Pr.*, **38**(1), 569-584.
- Computers and Structures, Inc. (2011), *CSI Analysis Reference Manual for SAP2000, ETABS, SAFE and CSI Bridge*, Berkeley, California, USA: Computers and Structures, Inc.
- Cruz, P.J. and Salgado, R. (2008), "Performance of vibration-based damage detection methods in bridges", *Comput. -Aided Civil Infrastruct. Eng.*, **24**(1), 62-79.
- Davis, T. (2013), "Algorithm 930: FACTORIZE: An object-oriented linear system solver for MATLAB", *ACM T. Math. Software*, **39**(4).
- Esfandiari, A., Bakhthiari-Nejad, F., Rahai, A. and Sanayei, M. (2009), "Structural model updating using frequency response function and quasi-linear sensitivity equation", *J. Sound Vib.*, **326**(1), 557-573.
- Ewins, D. J. (2000), *Modal Testing: Theory, Practice and Application*, 2nd Ed., Baldock, England: Research Studies Press.
- Fan, W. and Qiao, P. (2011), "Vibration-based damage identification methods: a review and comparative study", *Struct. Health Monit.*, **10**(1), 83-111.
- Fu, Y.Z., Lu, Z.R. and Liu, J.K. (2013), "Damage identification in plates using finite element model updating in time domain", *J. Sound Vib.*, **332**(1), 7018-7032.
- Gang, X., Chai, S., Allemang, J.R. and Lijun, L. (2014), "A new iterative model updating method using incomplete frequency response function data", *J. Sound Vib.*, **333**(1), 2443-2453.
- Garcia-Palencia, A.J. and Santini-Bell, E. (2013), "A two-step model updating algorithm for parameter identification of linear elastic damped structures", *Comput. - Aided Civil Infrastruct. Eng.*, TBD, **28**(7), 509-521.
- Garcia-Palencia, A.J., Santini-Bell, E., Sipple, J.D. and Sanayei, M. (2014), "Structural model updating of an in-service bridge using dynamic data", *Struct. Control Health Monit.*, **22**(10), 1265-1281.
- Gul, M. (2009), *Investigation of Damage Detection Methodologies for Structural Health Monitoring*, Ph. D. Dissertation, University of Central Florida, Orlando FL, USA.
- Gul, M. and Catbas, F.N. (2008), "Ambient vibration data analysis for structural identification and global condition assessment", *J. Eng. Mech. - ASCE*, **134**(8), 650-662.
- Hsieh, K.H., Halling, M.W. and Barr, P.J. (2006), "Overview of vibrational structural health monitoring with representative case studies", *J. Bridge Eng.*, **11**(6), 707-715.

- Jafarkhani, R. and Masri, S.F. (2011), "Finite element model updating using evolutionary strategy for damage detection", *Comput.-Aided Civil Infrastruct. Eng.*, **26**(1), 207-224.
- Kwon, K.S. and Ling, R.M. (2004), "Frequency selection method for FRF-based model updating", *J. Sound Vib.*, **278**(1), 285-306.
- Li, H., Huang, Y., Ou, J. and Bao, Y. (2011), "Fractal dimension-based damage detection method for beams with a uniform cross-section", *Comput.-Aided Civil Infrastruct. Eng.*, **26**(1), 190-206.
- Link, M. (1993), *Updating of analytical models—procedures and experience*, s.l., s.n., 35-52.
- Maia, N.M., Almeida, R.A., Urgueira, A.P. and Sampaio, R.P. (2011), "Damage detection and quantification using transmissibility", *Mech. Syst. Signal Pr.*, **25**(7), 2475-2483.
- MathWorks Inc. (2011), *Matlab Version 7.12 (R2011a)*, Natick MA, USA: s.n.
- Mendrok, K. and Uhl, T. (2010), "The application of modal filters for damage detection", *Smart Struct. Syst.*, **6**(2), 115-133.
- Modak, S.V. (2014), "Model updating using uncorrelated modes", *J. Sound Vib.*, **333**(1), 2297-2322.
- Mottershead, J.E. and Friswell, M.I. (1993), "Model updating in structural dynamics: A survey", *J. Sound Vib.*, **167**(2), 347-375.
- Mottershead, J.E., Link, M. and Friswell, M.I. (2011), "The sensitivity method in finite element model updating: A tutorial", *Mech. Syst. Signal Pr.*, **25**(1), 2275-2296.
- Panigrahi, S.K., Chakraverty, S. and Mishra, B.K. (2013), "Damage identification of multistory shear structure from sparse modal information", *J. Comput. Civil Eng.*, **27**(1), 1-9.
- Pascual, R., Golinval, J.C. and Razeto, M. (1996), "Testing of FRF based model updating methods using a general finite elements program", *Proceedings of the International Conference of Noise and Vibration Engineering ISMA21*.
- Rahmatalla, S., Eun, H.C. and Lee, E.T. (2012), "Damage detection from the variation of parameter matrices estimated by incomplete FRF data", *Smart Struct. Syst.*, **9**(1), 55-70.
- Rytter, T. (1993), *Vibration based inspection of civil engineering structure*, Ph. D. Dissertation, Aalborg University, Denmark.
- Talebinejad, I., Fischer, C. and Ansari, F. (2011), "Numerical evaluation of vibration-based methods for damage assessment of cable-stayed bridges", *Comput. - Aided Civil Infrastruct. Eng.*, **26**(1), 239-251.
- Thyagarajan, S.K., Schultz, S.J. and Pai, P.F. (1998), "Detecting structural damage using frequency response functions", *J. Sound Vib.*, **210**(1), 162-170.
- Tikhonov, A.N. and Arsenin, V.Y. (1977), *Solutions of Ill-Posed Problems*, New York: John Wiley & Sons.
- Wang, H. *et al.* (2014), "Finite element model updating of flexural structures based on modal parameters extracted from dynamic distributed macro-strain responses", *J. Intell. Mat. Syst. Str.*, Volume 1045389X14523856.
- Weber, B., Paultre, P. and Proulx, J. (2009), "Consistent regularization of nonlinear model updating for damage identification", *Mech. Syst. Signal Pr.*, **23**(6), 1965-1985.